Azimuth Angle Determination for the Arrival Direction of an Ultrasonic Echo Signal

Submitted: 10th January 2017; accepted: 18th April 2017

Bogdan Kreczmer

DOI: 10.14313/JAMRIS_2-2017/14

Abstract:

In the paper, an idea of a method of signal arrival direction estimation is presented. The influence of time error measurements on the usage of the method is described. An approach to the problem of an increase in the robustness of the method is proposed. The results of experiments are presented and discussed.

Keywords: *ultrasonic range finder, sonar, direction of arrival, azimuth angle*

1. Introduction

Commercial ultrasonic range finders, which are used as equipment for mobile robots, deliver very unreliable information. Their measurements are accurate in distance but their angular resolution is very poor. In order for this to improve, it is necessary to determine the direction of echo arrival (DOA). Considering the localization of an object by measuring the time of flight (TOF) of an echo signal and by determining its DOA, it is possible to distinguish two cases of this problem namely, 2-D and 3-D. In the 2-D case, only the azimuth angle is determined. To estimate the DOA in the 3-D case, the elevation angle needs to be computed. In this paper the 2-D case is considered. There are a lot of approaches to this task. Their important disadvantage is that they do not make it possible to create methods which, on the one hand, are not computationally expensive, and on the other hand, allow a compact device to be constructed by using popular ultrasonic transducers. To reduce this disadvantage, this paper proposes and analyzes a new approach to estimate the azimuth angle of a signal arrival direction. The main idea of the approach is based on exploiting a phase shift of a signal to determine the DOA. This idea is well known. The novelty of the presented approach is the method of applying this idea to this problem when the distance between receivers is bigger than half of a signal wavelength. The main idea of the approach was presented in [10, 11]. This paper extends the study regarding the DOA problem and presents experimental results that prove the effectiveness of the proposed method.

The paper is organized as follows: The next section introduces related works; In Section 3, the phase-shift approach to the problem of determining the signal arrival direction is discussed in relation to the distance between receivers; Section 4 describes the proposed method of an azimuth estimation that makes it possible to eliminate ambiguities caused by the fact that the inter-distance between receivers is bigger than a half wavelength of a signal; In Section 5, sources of measurement errors are discussed and their influence on the accuracy of the azimuth determination is described; Section 6 analyzes and evaluates the robustness of the proposed method; In Section 7, the results of experiments are presented and discussed; Section 8 gives the final conclusions.

2. Related Work

When using ultrasonic range finders to determine the DOA, a triangulation method based on the TOF can be applied. However, the paths of an emitted signal are different when it is reflected by a wall or rod. Therefore, such approaches combine the problems of object position determination and object recognition. Examples of this kind of approach to the 2-D case are the methods presented in [4, 8, 17]. They make it possible to distinguish planes and rods. Moreover, the methods described in [4, 8] are able to recognize a corner, which is understood as a concave intersection of two planes at right angles. The same features characterize the method presented in [14], which extends the approach described in [8] to the 3-D case. Analogous features for the 3-D case can also be found in the methods presented in [7, 16]. The accuracy of azimuth angle determination, reported in descriptions of the mentioned methods, is usually 1°. A common disadvantage of these approaches is that they result in the creation of sonar systems that are not compact in size. This problem was recognized in [21]. The proposed ultrasonic range finder consists of a single SensComp 600 electrostatic transmitter and four small microphones. The proposed sensor is compact in size but the distances between microphones are not small enough to guarantee that the received echos are produced by a signal reflected by the same object. To determine it, a mid point criterion is used. This criterion is a kind of simplification of a general criterion. Therefore, ambiguities can arise in some cases. To remove them, an additional fifth microphone can be added. The angle of the echo arrival direction is determined by exploiting the triangulation approach. To obtain very precise TOF measurements, a linear frequency modulated chirp with a bandwidth of 30 kHz and a duration of 512 μs was used. TOF is determined by computing a 1-bit correlation of a received echo and its template. The electrostatic transmitter SensComp 600 used in this construction has a big diameter (30 mm). It causes its directional pattern to have distinct side lobes. When an echo arrives from a direction outside a main lobe it is heavily changed. Therefore, instead of a sin-

gle echo template, the use of different templates that depend on direction are needed.

When using an array of receivers to estimate the DOA, the MUSIC (MUltiple SIgnal Classification) method can be used. In [20], this approach is used for locating a radio wave transmitter in an indoor environment. A wireless LAN router was used as the transmitter. The location of the transmitter is determined by exploiting several arrays of receivers that are located in different places. The same problem of determining the position of an object is considered in [3].

In [1], a mixed-signal full-custom VLSI chip is presented. It is designed to receive sonar return signals from an ultrasonic microphone array and also extract the input bearing angles of the incoming signals. The processing utilizes simple low-power analog spatiotemporal bandpass filters to extract wavefront velocity across the array, which translates to the input bearing angle. MEMS technology made it possible to create small size microphones. In [5], a linear array of MEMS microphones is presented. It was used for the implementation of beamforming algorithms and correlation function-based methods. The performed research showed that when the aim is to minimize the error of estimation of both the source angular position and distance, it is more reasonable to use methods that utilize the correlation function combined with delay-and-sum beamforming.

Spatial filters are also used in [19]. The presented method applies an array beamforming technique to the synthesis of 3-D spatial filters. By combining broadband beamforming with a sparse and random array of receivers, it was possible to obtain 3-D location measurements in the presence of multiple highly overlapping echos. Another approach, based on the processing of signals obtained from an array of receivers is presented in [6]. It is based on a cumulated signal amplitude in a single period. Because in this approach it is assumed that the maximal amplitude of a signal is the same during a long period of time, it is difficult to meet this assumption in practical implementation. In the considered paper, simulation results were only reported.

The discussed approaches for obtaining a very good accuracy of DOA determination involve relatively computationally expensive methods. The approach presented in this paper shows that it is possible to reduce the computational burden and to obtain a good accuracy of DOA estimation.

3. Determination of Signal Arrival Direction

Assuming that a signal source can be considered as a point with a uniform omni-directional pattern, the arrival direction can be determined by exploiting triangulation methods. In order to do this, at least two receivers are needed in which the acoustic axes are parallel to each other. To reduce the influence of error measurement on object localization and azimuth angle determination, receivers should be placed far enough away from each other. However, the bigger distance between receivers corresponds with a smaller probability that transducers receive a signal coming from the same source. Therefore, to increase this probability the receivers should be as close as possible to each other. It means that the triangulation method is not the best choice for this case.

While the distance between receivers is small in comparison to the distance to the signal source, the signal wave in the neighborhood of receivers can be treated as a planewave. To determine the incident angle of a signal wave, a transducer array consisting of two receivers (see Fig. 1) can be used. Assuming that

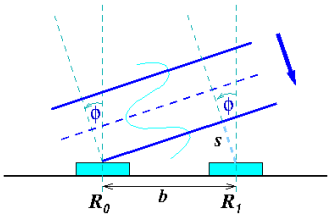

Fig. 1. A wavefront of a planewave propagated towards two receivers

a wavefront can be detected, it is possible to measure time t_{01}, which is an interval between the moment of a signal detection by the receiver R_0 and the moment of its detection by R_1. In this way, the following formula can be used to determine the incidental angle ϕ:

$$\phi = \arcsin \frac{s}{b} = \arcsin \frac{v_a t_{01}}{b}. \tag{1}$$

where s is the distance of a wavefront to the receiver R_1 at the moment when it reached the receiver R_0 (see Fig. 1), v_a is the speed of the acoustic wave and b is the distance between receivers R_0 and R_1.

3.1. Ambiguity of Phase Shift Determination

To determine the incident angle, Eq. 1 can be applied directly when the wavelength λ of the highest harmonic frequency of the signal meets the condition $b < \frac{\lambda}{2}$. If gap b is bigger, a phase shift cannot be correctly determined (see Fig. 2). It is due to the fact

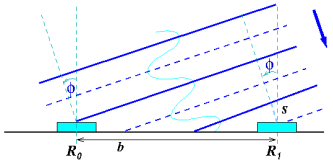

Fig. 2. A phase shift of a received signal for the case when a direct measurement gives a wrong result

that there are still some other possibilities of incident angles that result in the same measurement value of s (see Fig. 3). Popular piezoelectric transducers operate at a frequency of 40 kHz. In normal conditions the length of this wave is about 8.7 mm. It means that the distance between receivers cannot be larger than 4.35 mm. Unfortunately, commercially available transducers do not make it possible to meet this condition. Their common diameters are 10 mm, 12 mm, 14 mm

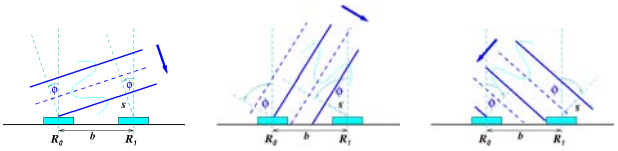

Fig. 3. Ambiguous results of the incident angle ϕ for the same value s

and 16 mm. The firm Knowles produces smaller receivers SPM0404UD5 with a size of about 4 mm. However, at this moment they are not very popular and easily available on the market.

When considering the influence of gap size on a set of ambiguous solutions of Eq. 1, it can be noticed that, in general, their number is increased by enlarging the gap every 0.5λ. This can vary, however, because it depends on a real incident angle ϕ for which other ambiguous solutions are determined. Figure 4 shows an example of a situation at which the correct incident angles are $0°$ and $30°$ respectively. The main horizontal lines represent the correct solution for a given gap size. For the incident angle $\phi = 0°$, ambiguous solu-

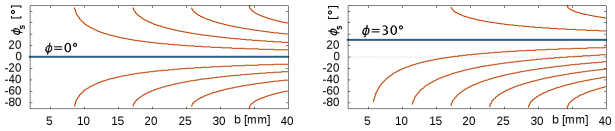

(a) (b)

Fig. 4. Ambiguous solution values ϕ_s in relation to the gap size between receivers for the incident angle ϕ equal to a) $0°$, b) $30°$

tions appear when $b > \lambda$. However, for $\phi = 30°$, the first ambiguous solution is obtained while $b \approx 0.65\lambda$. In the limit case for $\phi = 90°$, the first ambiguous solution appears when $b = 0.5\lambda$. The diagrams presented in Fig. 4 clearly indicate a bigger gap between receivers, more ambiguous solutions and that their values are closer and closer to each other.

3.2. Ambiguity Elimination

When comparing the diagrams in Fig. 4 it can be inferred that the angular range of unique solutions for a given gap size is not the same for all incident angle values. Due to the effective sensitivity ranges of the popular ultrasonic transducers being no wider than $[-70°, 70°]$, the examples presented in further analysis are restricted to that range. However, the final conclusions are also valid outside that range.

It is interesting which values of ambiguous solutions refer to the incident angle ϕ through the whole range of all possible angles ϕ and how they change. In Fig. 5 there are diagrams which gives the answer to this question. They show the values of possible solutions of Eq. 1 in relation to the values of the incident angle ϕ. The diagrams were computed for two gap sizes, namely 11 mm and 15 mm. The diagonals of each diagram reflect the correct values of the incident angle which correspond to the real values of that angle.

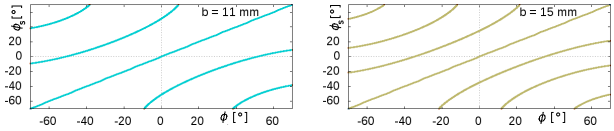

(a) (b)

Fig. 5. Values of possible solutions ϕ_s of Eq. 1 in relation to the values of the incident angle ϕ for the size of the gap b equal to a – 11 mm, b – 15 mm

The diagrams demonstrate that e.g. for the incident angle equal to $-20°$, using a pair of receivers with the gap $b = 11$ mm, a set of possible solutions of Eq. 1 is $\{-22°, 20°\}$. For the same angle and a pair of receivers with the gap $b = 15$ mm, a set of possible solutions is $\{-48°, -11°, 20°, 68°\}$. Interpretation of this case is shown in Fig. 6. It is easy to notice that a com-

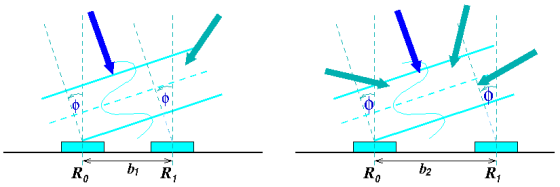

(a) (b)

Fig. 6. Examples of possible incident angles for measurement data obtained while the real incident angle is equal to $20°$. Directions were determined for the gap size b equal to a – 11 mm, b – 15 mm

mon part of these sets is the correct value of the incident angle. Thus, it indicates an approach which can be applied to this case. Instead of using a single pair of receivers, two pairs should be exploited. To make a receiver system more compact, one of the receivers of both pairs can be a common one. Finally, a transducer system consisting of three receivers is obtained (see Fig. 7). In this paper it is assumed that receivers

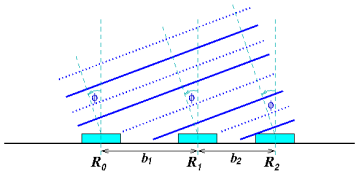

Fig. 7. Two pairs of receivers integrated into a single system of three transducers

are located in the horizontal plane as well as a signal source. Therefore the incident angle of the signal is the azimuth angle (see Fig. 8).

The discussed example of two receiver pairs clearly shows that in order to determine the correct value of an incident angle, both pairs have to have different gaps between their receivers. The only concern of that method is that the feature presented in the discussed example has to be preserved through the entire angular range of transducers sensitivity. In other words, the trajectories of possible solutions for both receiver pairs presented in Fig. 6 cannot cross each other. To

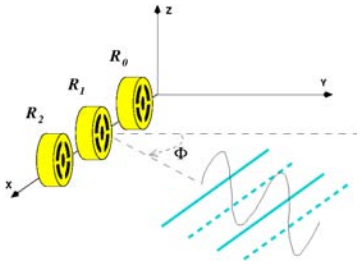

Fig. 8. Location of the sonar system in a 3-D coordinate system

be more precise, they cannot have any common part with each other. The only exception are the lines for correct solutions which have to be the common part of the both diagrams. Figure 9 shows that the combined solution sets determined for the two different receiver pairs have this feature. This example presents an ideal

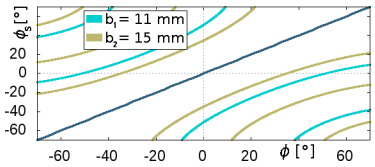

Fig. 9. Diagram of the combined solution sets determined for two cases of gap b equal to 11 mm and 15 mm

case which means that the measurement error is not taken into account.

4. Incident Angle Determination

Assuming that a signal has a narrow band, in a given moment it can be approximated by the following function

$$S(t) = A\sin(\omega t + \gamma),$$

where A is the amplitude of the signal, ω is its angular frequency and γ is the phase of the signal. When considering the 2-D case and the receivers' set presented in Fig. 7, a received signal by each transducer can be described in relation to R_0. In this way, the signal values measured by each receiver can be expressed as

$$\begin{cases} S_0(t) &= A\sin(\omega t + \gamma'), \\ S_1(t) &= A\sin(\omega t - k_x b_1 + \gamma'), \\ S_2(t) &= A\sin(\omega t - k_x(b_1 + b_2) + \gamma'), \end{cases}$$

where k_x is the x coordinate of the wave vector $\mathbf{k}$. To measure the delay of signal detection by each of the receivers, it is assumed that measurements are performed in relation to the receiver R_0. The procedure of the measurement performance can be activated when a signal received by all of the receivers reaches a given threshold value. Then, the measurements of the time delay of signals received by R_1 and R_2 start when a rising edge of a signal received by R_0 reaches the value 0. After that, the measurement performed by the receivers R_1 or R_2 is finished when a rising edge of a signal received by a respective receiver also reaches the value 0. Thus, we obtain measurements for two pairs of receivers, respectively $\{R_0, R_1\}$ and $\{R_0, R_2\}$. The measured intervals of time are written hereafter as t_{01} and t_{02}. Thus, they meet the following equations

$$\begin{cases} 0 &= A\sin(\omega t_{01} - k_x b_1), \\ 0 &= A\sin(\omega t_{02} - k_x(b_1 + b_2)). \end{cases} \tag{2}$$

Because the measurements are restricted to rising edges, Eq. 2 is equivalent to

$$\begin{cases} 2\pi n_1 &= \omega t_{01} - k_x b_1, \\ 2\pi n_2 &= \omega t_{02} - k_x(b_1 + b_2). \end{cases} \tag{3}$$

where n_1 and n_2 are integer numbers. Taking into account:

$$\omega = \frac{2\pi}{T_a} \quad \text{and} \quad k_x = \frac{2\pi\sin\phi}{\lambda} \quad \text{and} \quad \lambda = v_a T_a,$$

where T_a is a period of a received signal, Eq. 3 can be transformed into the following form

$$\begin{cases} n_1\lambda &= v_a t_{01} - b_1\sin\phi, \\ n_2\lambda &= v_a t_{02} - (b_1 + b_2)\sin\phi. \end{cases}$$

Both equations allow ϕ to be determined. The condition which binds them is that they have to give the same result

$$\begin{cases} \phi &= \arcsin\frac{v_a t_{01} - n_1\lambda}{b_1}, \\ \phi &= \arcsin\frac{v_a t_{02} - n_2\lambda}{b_1 + b_2}. \end{cases} \tag{4}$$

In this way, the problem of ϕ determination is reduced to the problem of finding the values of n_1 or n_2. When $b_1 \neq b_2$, the equations deliver redundant information that can be used to find the pair of correct values n_1 and n_2. It is worth noting that in this case a necessary condition which has to be met is

$$\frac{v_a t_{01} - n_1\lambda}{b_1} = \frac{v_a t_{02} - n_2\lambda}{b_1 + b_2}. \tag{5}$$

However, it is not a sufficient condition. Therefore, some ambiguities can arise. This problem was discussed in the previous section. As was previously shown, these ambiguities can be removed by setting the proper sizes of gaps b_1 and b_2. They also determine the range $[n_{min}, n_{max}]$ in which a correct pair (n_1, n_2) should be searched for. It allows the procedure of determination of the angle ϕ to be defined as follows:

1) Execute a signal emission and perform the measurements of t_{01} and t_{02}.
2) Find such a pair $n_1, n_2 \in [n_{min}, n_{max}]$ that meets the condition of Eq. 5.
3) Using formulas Eq. 4 determine ϕ.

To take into account errors of measurements the condition of Eq. 5 has to be transformed to the following form

$$\left|\frac{v_a t_{01} - n_1\lambda}{b_1} - \frac{v_a t_{02} - n_2\lambda}{b_1 + b_2}\right| < \varepsilon. \tag{6}$$

The value of ε is determined by the values of the errors of t_{01} and t_{02} measurements. Errors of b_1 and b_2 are systematic errors and they can be taken into account during a calibration procedure. Therefore, they are not considered here.

5. Sources of Errors

Accuracy of azimuth determination is degraded by measurement errors introduced by noise and a finite resolution of timer counters. The influence of noise on measurement results can be estimated by measuring the noise magnitude. The resolution of timers is known because of microcontroller settings. Inaccuracy of the location of a sensor also causes deviation in the final results. Fortunately, they are easy to eliminate by a calibration procedure. There is one more source of errors. In the presented approach it is assumed that a wave is flat. It is a common assumption in such a case. The assumption is very close to a real case when a signal source is far away. Unfortunately, when the sonar system is used in an indoor environment by e.g. a mobile robot, the differences between an ideal plane wave and a real one can be significant. The reason is that an encountered object can be located at a distance lower than 1 m. These differences create an error value of the discussed simplification. When following this line of reasoning, the time measurement error of a signal detection by the receiver R_1 in relation to the receiver R_0 can be expressed as follows

$$\Delta t_{01} = \Delta t_n + \Delta t_r + \tau$$

where Δt_n is an error caused by a noise, Δt_r is the resolution of a timer and τ is an error caused by the simplifying assumption that a received wave is a planewave.

There are also other sources of errors e.g. the leaking of signals between transducers (by air or by a sonar broad). However, results of experiments presented in Section 7 show that for the constructed sonar module the influence of such a phenomena on the accuracy of azimuth determination is very small or even negligible.

5.1. The Error of the Planewave Assumption

The value of the error τ depends on the source position in the distance and azimuth angle in relation to receivers. For the 2-D case it is assumed that the signal source is located in a plane determined by the receivers' acoustic axes. Therefore, it is enough to consider a wave propagated across the plain. While a signal is sent by a point-like source, it propagates as a spherical wave. Therefore, assuming that a signal is a plane wave, some receivers detect the signal a bit later in relation to the wavefront of a hypothetical plane wave. This difference creates an error caused by the simplifying assumption that a signal is a plane wave. Considering that the receiver's array consisted of the two transducers R_0 and R_1 and were placed at a distance d to the signal source S, the mentioned error is very close to the biggest one for the situation presented in Fig. 10. In this case, it is assumed that the wavefront of a propagated planewave is parallel to the baseline of receivers. It means that $s = 0$ (compare with Fig. 1). Assuming that a wave is a plane one, the receiver R_1 receives a signal a bit later than is expected. The delay of a wavefront detection is

$$\tau = \frac{\Delta s}{v_a}$$

where Δs is the distance between the wavefront of the hypothetical planewave and the wavefront of the real spherical one and v_a is the speed of an acoustic wave. When exploiting simple geometric dependencies, Δs

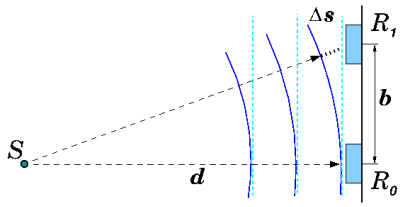

Fig. 10. An error value of a spherical wave approximation by a plane wave for the sonar system consisting of two receivers and located in a horizontal plane

is expressed by the following formula

$$\Delta s = \sqrt{d^2 + b^2} - d \approx \frac{b^2}{2d} \quad \text{for} \quad d \gg b. \qquad (7)$$

where b is the distance between the receivers and d is the distance between the signal source S and the receiver R_0. In this case, the distance Δs is the error of the simplifying assumption that transducers receive a planewave. Eq. 7 confirms the intuitive expectation that the error is decreased when a source distance is increased. Examples of a Δs value change in relation to the distance to a source are shown in Fig. 11. There are two diagrams for the two values of gap b, namely 11 mm and 22 mm. For distance ranges of above 0.5 m,

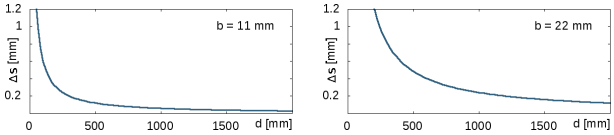

Fig. 11. Diagrams of the Δs change in relation to the distance to a signal source

these examples show that the error Δs is rapidly decreased. Because the error is approximately proportional to the squared gap b between receivers, the double increase of b results in four times an increase of Δs (see Fig. 11a and Fig. 11b). The impact of b on the error Δs is diminished by a distance increase (compare Fig. 12a and Fig. 12b). To the express values of the er-

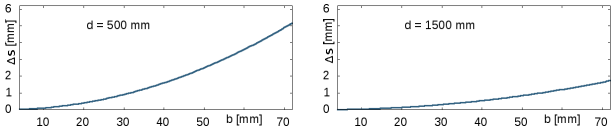

Fig. 12. Diagrams of the Δs change in relation to the size of gap b for distances to a signal source that are equal to 0.5 m and 1.5 m respectively

ror Δs in a time domain, it is enough to say that 1 mm is equal to about $2.92\ \mu s$.

The presented examples show that when b is no larger than about 30 mm, the error Δs does not seem

to be big for signal sources placed at a distance of 0.5 m or greater. Therefore, they justify the simplification that an echo is a planewave. For this case, the following relation can be assumed:

$$\Delta t_{01} \simeq \Delta t_n + \Delta t_r.$$

Considering that the system consisted of the two receiver pairs presented in Fig. 7 for which b_1 and $b_2 < 30$ mm, it can be assumed that the error of time measurement is the same for both pairs. Therefore, from now the notation Δt will be used.

5.2. Inaccuracy of Azimuth Determination

To determine the impact of time measurement Δt on the accuracy of the azimuth ϕ determination, Eq. 1 can be exploited. Using differential calculus to approximate the error of determination of the incident angle ϕ in respect to Δt, the following formula is obtained

$$\Delta\phi = \frac{v_a}{b\sqrt{1 - sin^2\phi}}\Delta t. \tag{8}$$

To exemplify this relation, diagrams are presented in Fig. 13. They show the approximations of error values of ϕ determination for two sizes of gap b, namely 4 mm and 12 mm. The computations were performed under the assumption that $\Delta t = 1\ \mu s$. It is worth noting that

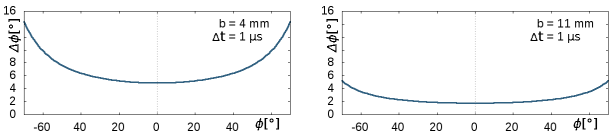

Fig. 13. Diagrams of approximations of the error $\Delta\phi$ of the incident angle ϕ determination. The diagrams present the error $\Delta\phi$ for $\Delta t = 1\ \mu s$ and two values of gap b. They are 4 mm and 11 mm respectively.

the value of the error $\Delta\phi$ increases while the azimuth grows. It can be noticed that the error $\Delta\phi$ is reduced while the size of gap b is bigger. This is because $\Delta\phi$ is inversely proportional to b. In Fig. 14 it is shown in a more distinct way.

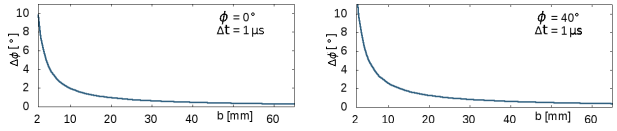

Fig. 14. Diagrams of approximations of the error $\Delta\phi$ of incident angle ϕ determination in relation to the size of gap b. The diagrams present the error $\Delta\phi$ for $\Delta t = 1\ \mu s$ and two values of the incident angle ϕ. They are $0°$ and $40°$ respectively.

6. Robustness

When taking into account Eq. 8 and estimating Δt by a given value, it is possible to determine $\Delta\phi$ in the entire range of all possible values of the azimuth angle ϕ. In this way, irregular stripes are obtained instead of the curves presented in Fig. 9. The diagram shown in Fig. 15a demonstrates the case when the error of time measurement Δt is 2 μs. The stripes that represent possible solutions are narrow and a bit wider at their ends. This is coherent with the previous analysis and the examples presented in Fig. 13. The obtained

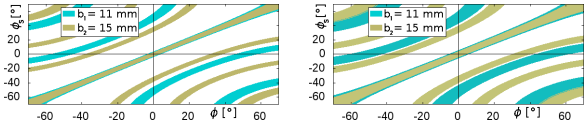

Fig. 15. Diagrams of the combined solution sets determined for two cases of gap b equal to 11 mm and 15 mm. It includes the measurement error influence on the possible values of determined angles. It is assumed that the measurement error of signal detection is a – 2 μs, b – 3 μs

result shows that the stripes, which represent other angles than the correct ones, do not have a common part. This feature suggests that it is possible to obtain the correct determination of the azimuth angle ϕ. By increasing the error value up to 3 μs, a limit for this configuration of receivers is reached. The areas of different solutions are no longer separated (see Fig. 15b).

6.1. Reducing Baseline

To increase the robustness of the system, the distance b for one of the receiver's pairs should be reduced. Taking into account the previous assumption that a signal wave is a planewave and propagated in a plain determined by the receivers' acoustic axes, it is possible to arrange a system of three receivers in a slightly different way. Instead of putting them along a single line, one of them can be moved a bit above (see Fig. 16). It allows an effective distance in a horizontal

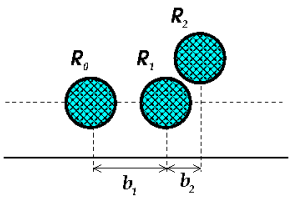

Fig. 16. Arrangement of three receivers with a reduced horizontal gap

line to be reduced below their diameters. In this way, the receivers' system is obtained. The system is more robust and the error of 3 μs is accepted. Assuming that the effective distance between T_2 and T_3 is 4 mm, a single stripe of the possible solutions of Eq. 1 is obtained.

6.2. Robustness Estimation

The separation of stripes representing different values of ϕ is the necessary condition of finding the correct solution. However, it is not the sufficient condition. Therefore, the diagrams presented in the previous subsection do not make it possible to properly estimate the biggest acceptable error value that does not cause misinterpretation of measurement results. This is because Eq. 6 can be met by the values of n_1 and

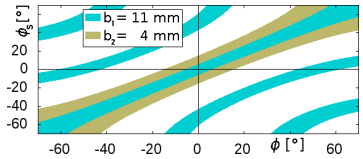

Fig. 17. Diagram of the combined solution sets determined for two cases of gap b equal to 11 mm and 4 mm. It includes the measurement error influence on the possible values of the determined angles. It is assumed that the measurement error of signal detection is 3 μs

n_2, which represent different and not overlapping stripes. The reason is that Eq. 6 determines the distance between these points. In Fig. 18 there are two pairs of points namely $\{P_{n_1}, P_{n_2}\}$ and $\{P_{n_1'}, P_{n_2'}\}$ which correspond to the pairs of values n_1, n_2 and also $n_1^{'}$, $n_2^{'}$ respectively. The distance between these points is the

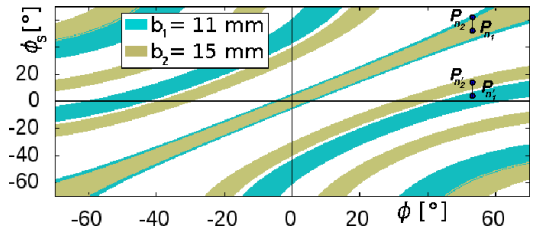

Fig. 18. The condition expressed by Eq. 6, which refers to the distance between points that correspond to the pairs of values n_1 and n_2

same. Thus, if Eq. 6 is met for the pair $\{P_{n_1}, P_{n_2}\}$ it will also be met for the second pair. However, the pair $\{P_{n_1'}, P_{n_2'}\}$ does not represent the correct solution.

In order to determine an acceptable value of Δt and, then, the value of ε, the following computational procedure has been implemented:

1) For all directions $\phi_i \in [\phi_{min}, \phi_{max}]$
   - Compute t_{01} and t_{02} for a given direction ϕ_i
   - For all $\Delta t_i, \Delta t_j \in [-\Delta t, \Delta t]$
     - Determine n_1 and n_2 for $t_{01} + \Delta t_i$ and $t_{02} + \Delta t_j$.
     - If a solution is not found, increase ε and go to step 1).
     - If a solution is not unique, take the previous values ε and Δt for which computation for all directions succeeded. Return the values ε and Δt as the result and then stop.
     - Otherwise continue the loop.
2) Increase Δt and go to step 1).

Using this procedure, computations were performed for a few sets of gaps b_1 and b_2. The results are presented in Tab. 1. The minimal value of an angle determination error (min $\Delta\phi$) is obtained for directions $\phi = 0°$. The maximal value of that error is reached at the borders of the considered angle range. This is the consequence of Eq. 8 which is illustrated in the diagram presented in Fig. 13.

Tab. 1. Results of robustness analysis

b_1, b_2 [mm]	11, 15	11, 4	4, 11	4, 11
range: ϕ [°]	±50	±50	±60	±50
ε	0.05	0.08	0.4	0.3
Δt_{01} [μs]	**±0.9**	**±1.4**	**±1.5**	**±2.5**
min $\Delta\phi$ [°]	±1.2	±2.2	±4.7	±7.8
max $\Delta\phi$ [°]	±1.8	±3.5	±11.4	±14.4

When the range of the considered incident angles is extended, the acceptable error of time measured is reduced in spite of an increase of ε. This is due to the increase of an error of incident angle determination at the boundary of the range of the considered angles (see Fig. 13).

7. Experiments

In the presented experiment, measurements to a wall were performed. The benefit of using such an object is that the reflected signal produces a strong echo. Therefore, the object is detectable by a sonar in a wide range of angles of sonar orientation in relation to the object. It is well known that when the irregularities of an object surface are much smaller than the wavelength of a signal, the signal is reflected by this surface like light by a mirror. Therefore, despite of the orientation of a sonar module, the echo of the emitted signal arrives in each case from the direction which is perpendicular to the surface of the wall. A sketch of this phenomena is presented in Fig. 19. The sonar module

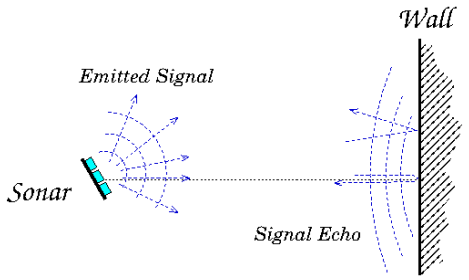

Fig. 19. Signal path

used in the experiment was equipped with popular piezoelectric ultrasonic transducers (see Fig. 20(a)). Four receivers are contained in this construction but in the discussed experiment only three of them were used. The module was mounted on a scanning device (see Fig. 20(b)) which made it possible to change the module orientation by $1°$. The frequency of the emitted signal was about 40 kHz. It means that the wavelength of the signal is 8.7 mm. The irregularities of the wall's surface were far below 1 mm. It therefore means that this case meets the conditions of the described phenomena (see Fig. 19). With this fact in mind and by choosing the local coordinate system of the sonar module and the global one in the way presented in Fig. 21, it is clear that the relation between the angle α of the sonar module orientation and the azimuth angle

(a) (b)

Fig. 20. Devices used in the experiment a – a sonar module, b – a sonar scanner consisting of a sonar module and a scanning device

(a)

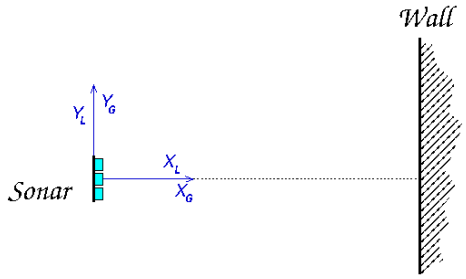

(b)

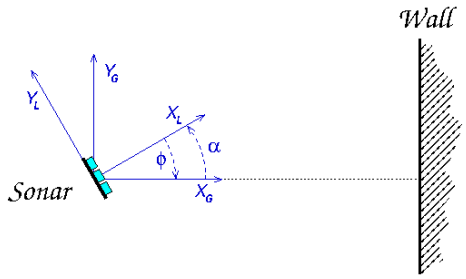

Fig. 21. Coordinate systems chosen for the experiment a – the origins of the local and global coordinate systems are placed in the middle of the sonar module, b – the azimuth angle ϕ measured in the local coordinate system has an opposite sign to the rotation angle α measured in the global coordinate system.

ϕ of the direction of signal arrival is

$$\phi = -\alpha. \tag{9}$$

The range of the sonar module orientation change was set to $[-50°, 50°]$. Eq. 9 means that the ideal measurement results should create a diagonal of the diagram frame that is shown in Fig. 22.

The real measurement data was obtained for a wall by placing the sonar scanner at distances of 1 m, 1.5 m, and 2 m. It was done in a corridor where there was enough long flat wall available (see Fig. 23). Using this data, the directions of signal arrival were determined by using the presented method. The parameter ε was set to 0.3.

The distance was determined by applying the threshold method. The obtained results are typical for this kind of method (see Fig. 24). Similar results are obtained for other range finders that exploit the same

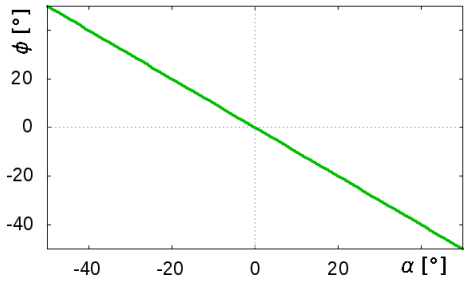

Fig. 22. The diagram of the ideal results determined by Eq. 9

Fig. 23. Location of the rotary sonar system in relation to the wall

method e.g range finders using electrostatic ultrasonic transducers [12]. This is the most simple approach. It does not guarantee the obtaining of accurate results when the range finder orientation to an object changes. However, in this experiment the main point was to determine the azimuth of an echo arrival rather than the distance. Nevertheless, the observed changes of measured distance in the wide orientation range $[-40°, 40°]$ were not bigger than 5 cm which seems to be a good result for such a simple method. Each measurement was performed 10 times. For each set of measurements the standard deviation σ was computed. In this experiment, the measurement error was presupposed 3σ plus the error caused by the timer's finite resolution. The mentioned resolution was 0.33 μs. The measurement errors were below 1 mm for a lot of the module orientations. Therefore, for such cases it was not possible to mark them in Fig. 24. The determined values of the azimuth angle are presented in Fig. 25. For nearly the whole range of orientation changes of the sonar module, the determined values are very close to the expected ones depicted as the diagonals of the diagrams. In the range $[-20°, 20°]$ the accuracy is very good. The error values of the measurements determined as 3σ were below $2°$.

Information concerning echo arrival direction significantly increases the reliability of data interpretation. Fig. 26 shows a popular representation of measurement results for ultrasonic range finders. Because these range finders do not deliver any other information apart from distance, in this interpretation it is assumed that an object to which a distance is measured is located ahead of the range finder. To improve data interpretation, Moravec and Elfes in [15] proposed a

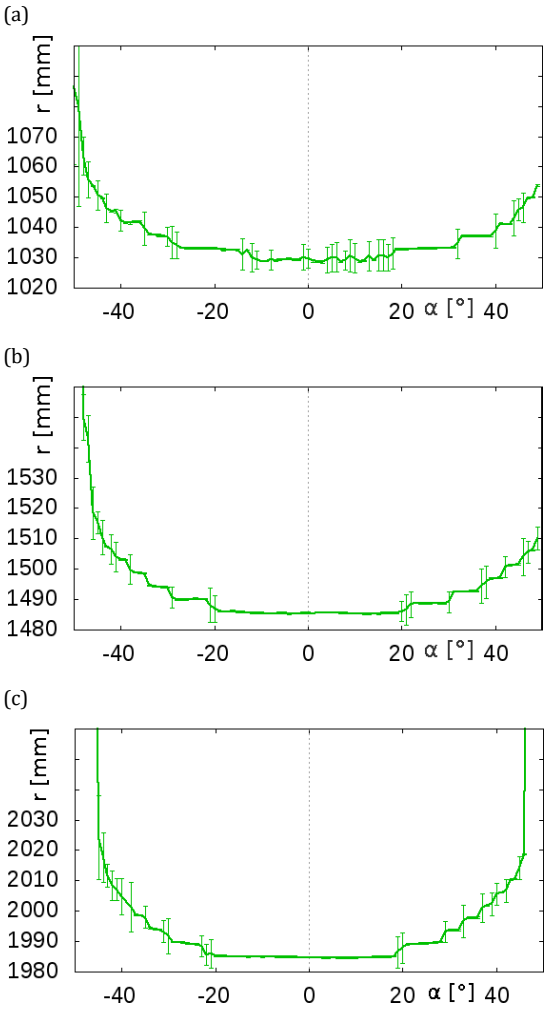

Fig. 24. Results of distance measurements for a wall at distances:
a – 100 cm, b – 150 cm, c – 200 cm

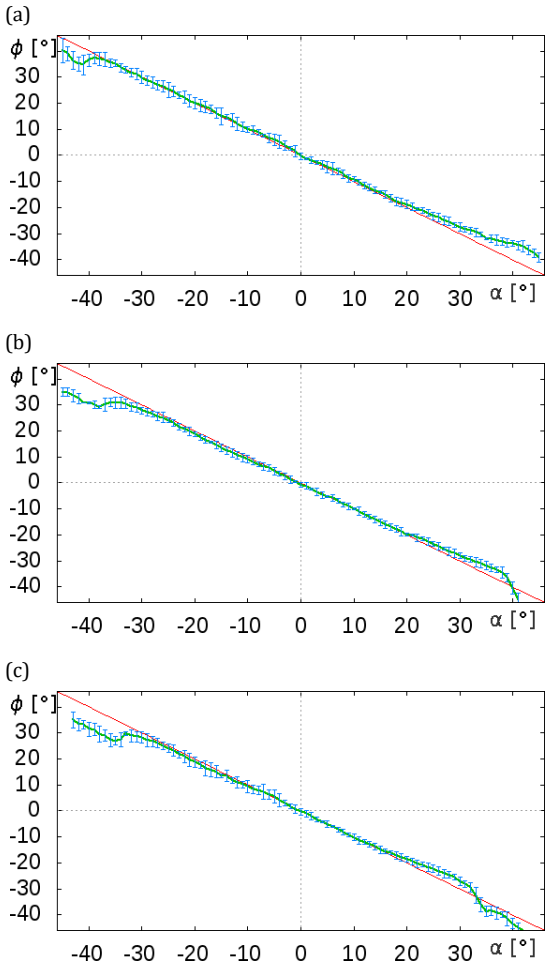

Fig. 25. Results of azimuth measurements for a wall at distances:
a – 100 cm, b – 150 cm, c – 200 cm

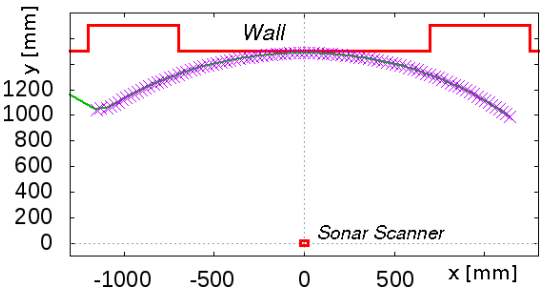

Fig. 26. A naive representation of measurement results obtained from the sonar scanner

probabilistic approach to the description of area occupancy by an object. This idea was exploited by many researchers in their work on mobile robot navigation using ultrasonic range finders e.g. in [2,13,18]. However, it never succeeded in building an effective navigation system for a mobile robot. Therefore, it seems that improvement of interpretation reliability of obtained data is the key problem.

The size of the change when information of echo direction arrival is available can be noticed by comparing Fig. 26 and 28. All determined points are close to the real point of signal reflection. The errors of azimuth determination cause a smearing of the point location by creating a kind of line segment along the wall (see Fig. 27). However, when restricting the data to the range $[-20°, 20°]$ in which the obtained results are much more accurate, the image of this case is far closer to the real situation and definitely gives more reliable information about the localization of an object. The decrease in accuracy of azimuth determination while the angle of direction arrival increases is consistent with Eq. 8. The diagrams presented in Fig. 13 show that the error of azimuth determination increases rapidly with the increase of the azimuth angle. The experiment measurements are restricted to the range in which the increase of the error is rather moderate. Nevertheless, it is noticeable.

8. Conclusion

The important advantage of the presented approach is that it makes it possible to use popular piezoelectric ultrasonic transducers to construct the module of a range finder with the ability to determine the azimuth angle of echo arrival in a wide range of angles. Because of this ability the module in this paper is called a sonar instead of a range finder. The proposed

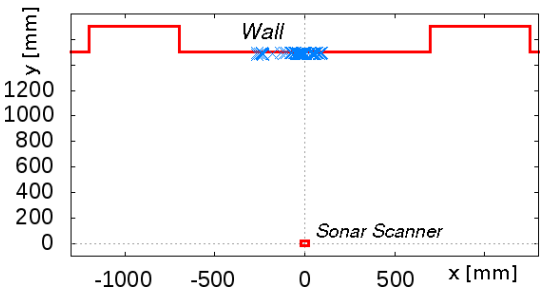

Fig. 27. Representation of measurements obtained from the sonar scanner which takes into account information of the direction of the echo arrival

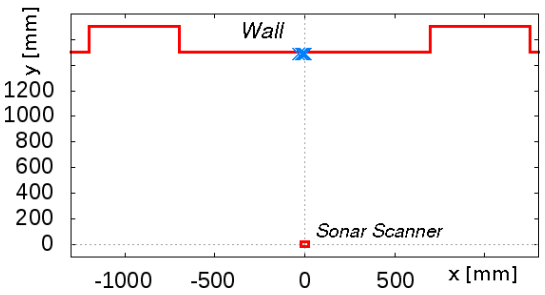

Fig. 28. Representation of measurements obtained from the sonar scanner in the range $[-20°, 20°]$ ***of its orientation change***

method determining the signal arrival direction is not very computationally expensive and can be implemented on a microcontroller. The error analysis shows that the method is not very robust. The accepted error of time measurement is about 2 μs. However, the created sonar module seems to be far below this requirement. In spite of the very simple construction of this module, the obtained experimental results prove that it is possible to reach a very good accuracy of determination of the echo azimuth. The presented examples show how a dramatic change in the reliability of ultrasonic ranging data interpretation has been achieved by the determination of the azimuth of echo arrival.

It seems that it is possible to increase the robustness of the method. This extension should also make it possible to increase the accuracy of azimuth determination. This is the goal of further work.

In the presented approach it is assumed that for a period of time during which a measurement is performed, a received echo comes from a single object. In other words, the effect of interference of echos arriving from different directions is not considered. When echos interfere, it can be expected that false results will be obtained. A preliminary study on this subject performed in [9] shows that results of DOA determination for such a case has a good feature. It means, when echos arriving from two directions are received, their interference still makes it possible to determine a direction. In this case, it is somewhere between these two directions. The final result depends on echos' amplitudes. The determined direction is closer to an echo's direction in which the amplitude is bigger.

ACKNOWLEDGEMENTS

This work was supported by the European Commission (EC), Polish Ministry of Science and Higher Education and was funded by the EU FP7 ICT-610902 project ReMeDi (Remote Medical Diagnostician) and the Polish funds for science in the years 2014 – 2016 granted to a cofinanced international project.

AUTHOR

Bogdan Kreczmer – Department of Cybernetics and Robotics, Faculty of Electronics, Wrocław University of Science and Technology, ul. Janiszewskiego 11/17, 50-370 Wrocław, Poland, e-mail: bogdan.kreczmer@pwr.edu.pl.

REFERENCES

[1] M. A. Clapp and R. Etienne-Cummings, "Single ping-multiple measurements: sonar bearing angle estimation using spatiotemporal frequency filters", *Circuits and Systems I: Regular Papers, IEEE Transactions on*, vol. 53, no. 4, 2006, 769–783, 10.1109/TCSI.2005.859613.

[2] I. Cox and J. Leonard, "Probabilistic data association for dynamic world modeling: A multiple hypothesis approach". In: *Proc. Fifth Int. Conference on Advanced Robotics*, Pisa, Italy, 1991, 1287–1294, 10.1109/ICAR.1991.240377.

[3] A. Harter, A. Hopper, P. Steggles, A. Ward, and P. Webster, "The anatomy of a context-aware application". In: *Proceedings of the 5th Annual ACM/IEEE International Conference on Mobile Computing and Networking*, New York, NY, USA, 1999, 59–68, 10.1145/313451.313476.

[4] A. Heale and L. Kleeman, "Fast target classification using sonar". In: *Intelligent Robots and Systems, 2001. Proceedings. 2001 IEEE/RSJ International Conference on*, vol. 3, 2001, 1446–1451, 10.1109/IROS.2001.977184.

[5] K. Herman, T. Gudra, and J. Furmankiewicz, "Digital signal processing approach in air coupled ultrasound time domain beamforming", *Archives of Acoustics*, vol. 39, no. 1, 2014, 27–50, 10.2478/aoa-2014-0005.

[6] A. Im, M. Gialich, Z. Aliyazicioglu, and H. K. Hwang, "DOA estimation via phase measurement". In: *Progress In Electromagnetics Research Symposium*, Taipei, Taiwan, 2013, 453–457.

[7] J. Jimenez, M. Mazo, J. Urena, A. Hernandez, F. Alvarez, J. Garcia, and E. Santiso, "Using PCA in time-of-flight vectors for reflector recognition and 3-D localization", *Robotics, IEEE Transactions on*, vol. 21, no. 5, 2005, 909–924, 10.1109/TRO.2005.851375.

[8] L. Kleeman and R. Kuc, "Mobile robot sonar for target localization and classification", *Int. J. Robotics Res.*, vol. 14, no. 4, 1995, 295–318, 10.1177/027836499501400401.

[9] D. Koszkul. "Object localization in a robot environment by using a system of ultrasonic range finder modules". Master's thesis, Wrocław University of Science and Technology, 2016.

[10] B. Kreczmer, "Determination of arrival direction of an ultrasonic signal for 2-D case". In: K. Tchoń and C. Zieliński, eds., *Postępy robotyki*, 2016, 303–312, (in Polish).

[11] B. Kreczmer, "Phase shift determination for azimuth angle estimation of echo arrival direction". In: *21st International Conference on Methods and Models in Automation and Robotics (MMAR)*, 2016, 1076–1081, 10.1109/MMAR.2016.7575287.

[12] R. Kuc, "Pseudoamplitude scan sonar maps", *IEEE Trans. Robot. Automat.*, vol. 17, no. 5, 2001, 787–770, 10.1109/70.964675.

[13] J. J. Leonard and H. F. Durrant-Whyte, "Mobile robot localization by tracking geometric beacons", *IEEE Trans. Robot. Automat.*, vol. 7, no. 3, 1991, 376–382, 10.1109/70.88147.

[14] H. M. Li and L. Kleeman, "A low sample rate 3D sonar sensor for mobile robots". In: *Robotics and Automation, 1995. Proceedings, 1995 IEEE International Conference on*, vol. 3, 1995, 3015–3020, 10.1109/ROBOT.1995.525712.

[15] H. P. Moravec and A. Elfes, "High resolution maps from wide angle sonar". In: *Proc. 1985 IEEE Int. Conf. Robot. Automat.*, 1985, 116–121, 10.1109/ROBOT.1985.1087316.

[16] A. Ochoa, J. Urena, A. Hernandez, M. Mazo, J. Jimenez, and M. Perez, "Ultrasonic multitransducer system for classification and 3-D location of reflectors based on pca", *Instrumentation and Measurement, IEEE Transactions on*, vol. 58, no. 9, 2009, 3031–3041, 10.1109/TIM.2009.2016820.

[17] H. Peremans, K. Audenaert, and J. M. V. Campenhout, "A high-resolution sensor based on triaural perception", *IEEE Trans. Robot. Automat.*, vol. 9, no. 1, 1993, 36–48, 10.1109/70.210793.

[18] B. Schiele and J. L. Crowley, "Certainty grids: Perception and localisation for a mobile robot". In: *Proc. the Int. Workshop on Intelligent Robotic Systems'93*, Zakopane, 1993, 159–165.

[19] J. Steckel, A. Boen, and H. Peremans, "Broadband 3-D sonar system using a sparse array for indoor navigation", *Robotics, IEEE Transactions on*, vol. 29, no. 1, 2013, 161–171, 10.1109/TRO.2012.2221313.

[20] J. Terada, H. Takahashi, Y. Sato, and S. Mutoh, "A novel location-estimation method using direction-of-arrival estimation". In: *Vehicular Technology Conference, 2005. VTC-2005-Fall. 2005 IEEE 62nd*, vol. 1, 2005, 424–428, 10.1109/VETECF.2005.1557946.

[21] C. Walter and H. Schweinzer, "Locating of objects with discontinuities, boundaries and intersections using a compact ultrasonic 3D sensor". In: *2014 International Conference on Indoor Positioning and Indoor Navigation*, 2014, 99–102, 10.1109/IPIN.2014.7275532.